Fully integrated optical isolators for space division multiplexed (SDM) transmission

Yongmin Jung,[1] Andrew Wood,[1] Saurabh Jain,[1] Yusuke Sasaki,[2] Shaif-Ul Alam,[1] and David J. Richardson[1]

[1]*Optoelectronics Research Centre, University of Southampton, Southampton, SO17 1BJ, U.K.*

[2]*Fujikura Ltd., 1440, Mutsuzaki, Sakura, Chiba, 285-8550, Japan*

A micro-optic collimator assembly represents an important platform for the realization of many commonly used fiber optic components and devices including optical isolators, circulators, gain flattening filters and so on. In this paper, we investigate the incorporation of SDM fibers (particularly, few mode fibers and multicore fibers) in a micro-optic collimator assembly and develop a technology base to provide fully integrated SDM components. A few exemplary SDM fiber isolators (e.g. 3 or 6-moded fiber isolator and a 32-core multicore fiber isolator) are successfully fabricated with low insertion loss and low mode (or core) dependent losses. Improved sharing of the functional optical element and significant device integration is efficiently achieved in these devices as will be required to ultimately realize the anticipated cost reduction benefits of SDM technology.

I. INTRODUCTION

Space division multiplexing (SDM) [1–3] utilizing few-mode fibers or multicore fibers supporting multiple spatial channels, is currently under intense investigation as an efficient approach to overcome the current capacity limitations of high-speed long-haul transmission systems based on single mode optical fibers. Unlike widely used single-mode fiber systems, however, the essential components needed to build SDM systems are still not commercially available and the basic prototype systems used in many experiments to date have been implemented only with the aid of bulky free-space optical components [4–6]. These are not only bulky but also expensive and tend to introduce high optical losses. From this perspective, a fiber-optic approach will inevitably be the preferred route forward and the fabrication of fully fiberized components is a pre-requisite for realizing practical SDM systems. An optical fiber collimator (i.e. fiber optic collimation and focusing assembly) represents an important platform for the realization of many commonly used fiber optic components and devices including optical isolators, circulators, gain flattening filters, WDM couplers, switches and variable optical attenuators. Current micro-optic collimators usually use GRIN lens or C-lens elements to transform the light from an input single mode optical fiber into a collimated free space beam and to refocus it into an output single mode fiber in a compact and cost effective manner [7]. In this paper, we investigate the incorporation of SDM fibers (e.g. few mode fibers and multicore fibers) in a micro-optic collimator assembly and investigate the feasibility of demonstrating SDM fiber optic components for SDM transmission, note provisional results

were reported in [8,9]. Due to the simple fabrication process, good beam transfer quality and low cost, these devices represent an extremely attractive means to reduce the cost of building and operating SDM systems.

II. FEW MODE FIBER ISOLATORS

Figure 1(a) shows a schematic diagram of a few-mode fiber (FMF) isolator assembly consisting of a cylindrical micro-optic lens and a few mode fiber ferrule, fitted in a ferrule sleeve [8]. Compact fiber optic collimators usually use C-lens (or GRIN lens) elements to transform the emergent light from an input FMF into a collimated free-space beam that can then be refocused into another length of FMF using a second identical assembly operated in reverse. In order to minimize Fresnel reflection, the few-mode fiber was angle-cleaved at an 8^o angle (or polished for a higher-quality surface) and a C-lens was prepared with both anti-reflection coatings and an 8^o facet angle. The C-lens was first carefully inserted into the ferrule sleeve and fixed with UV curable adhesive. The few-mode fiber ferrule was then inserted into the other end of the ferrule sleeve and the distance between the C-lens and fiber ferrule was carefully adjusted to achieve the best quality collimated beam (i.e. minimum beam spread). Generally, the beam divergence angle of the higher-order modes will be larger than that of the lower-order modes and so the far-field intensity profile of the higher order modes was monitored with a charge-coupled device (CCD) to identify the minimum beam spot size. If the distance between the lens and fiber end is too small the beam will diverge. Conversely, for too large distance it converges. Therefore, for the far field measurement, the minimum beam spot size ensures that the fiber is effectively placed at the focal point of the lens. It is interesting to note that the effective focal length of the lens used in this experiment was very short (f=2.98 mm) and that deflection caused by the angled fiber output was negligible meaning that orientation of the angled fiber facet was not particularly critical. In our experiment, a graded-index two-mode group fiber (OFS Fitel Denmark) was used as the exemplary few mode fiber. Firstly, the beam diameter at the far field position was measured as a function of distance from the collimator at a wavelength of 1550 nm. As shown in Fig. 1(b), the two spatial modes supported (LP_{01} and LP_{11}) both remain reasonably well collimated over a large distance (up to 50 mm) from the collimator. The beam diameter is defined as the distance across the center of the beam for which the intensity equals $1/e^2$ of the maximum and the beam diameters are in the range of 320-410 μm for LP_{01} and 450-730 μm for LP_{11} as the distance varies from 10 mm to 50 mm. Note that the LP_{11} mode has a bigger mode field diameter and its beam divergence was larger than that of the LP_{01} mode and this tends to result in a relatively higher insertion loss for the LP_{11} mode relative to the LP_{01} mode. In order to measure the mode dependent coupling loss of a pair of FMF collimators, each collimator assembly was mounted on a five-axis precision micro-stage to align the collimators and a mode selective multiplexer based on phase plates was employed to generate pure spatial modes (modal purity > 20 dB) at the input end of the FMF. A 1550 nm Fabry-Perot laser diode and a power meter were used for optical power measurements as a function of working distance. For the LP_{01} mode, as shown in Fig. 1(c), the total

coupling loss from a pair of FMF collimators was only 0.7 dB at a working distance (L) of 10 mm (including the insertion loss of the collimator itself) and it gradually increased to 0.8 dB and 1.1 dB at L=30 mm and 50 mm, respectively. For the LP_{11} mode, the coupling loss was 1.0 dB at L=10 mm and it increased more rapidly to 1.5 dB and 2.8 dB at L=30 mm and 50 mm, respectively. As expected from the far-field spot size measurement in Fig. 1(b), it is apparent that the LP_{11} mode has a higher coupling loss than LP_{01} mode due to the increased beam divergence. However note that the mode dependent loss (MDL) of the device was quite small (only 0.3 dB at L=10 mm and 0.7 dB at L=30 mm) and consequently the device is suitable for SDM transmission applications, where one of the most important requirements for passive optical components is a low MDL. The working distance range from 10 mm to 30 mm is long enough to allow the incorporation of most functional optical elements in the free space region between the two collimators and it can provide a compact and simple platform to develop integrated passive optical components for SDM applications.

Another important optical property of the device is the modal crosstalk. Low modal crosstalk is necessary for realizing mode-selective SDM transmission and a time-of-flight measurement (i.e. temporal impulse response) was used to characterize the modal content over a 10 km length of FMF including a pair of FMF collimators at the input end of the spool. The modal extinction ratio (ER) of our mode multiplexer was more than 20 dB at the input end and we can measure the degradation of the modal purity from the FMF collimator if it induces higher levels of modal crosstalk. As shown in Fig. 2(a), a high ER can be preserved for the LP_{11} across the pair of FMF collimators, however the ER of the LP_{01} mode was slightly degraded to -16.8dB. We believe that this is associated with a non-ideal working distance between the two collimators and further ER optimization is under investigation using a telecentric optical configuration. In order to demonstrate the feasibility of SDM components, an optical isolator core was incorporated between the two FMF collimators. When a single stage, polarization-insensitive optical isolator core was inserted between the collimators the coupling loss was increased by about 0.1 dB for each spatial mode and the peak optical isolation was 43 dB at 1559 nm and the isolation exceeded 32 dB over the full C-band as shown in Fig. 2(b). Higher levels of optical isolation could easily be achieved using a dual-stage optical isolator core. We also measured the back reflection from FMF collimators and a value of -32dB was obtained over full-C band due to the angled fiber facet. Further reduction could easily be achieved by applying an anti-reflection coating on the surface of the FMF end facet. These results indicate that a great variety of free space optical components can be integrated in FMF collimators ensuring the same optical function can be simultaneously achieved for all spatial channels with nearly identical performance. The current device demonstration has been mainly focused on two port devices having a single input and a single output, however it also can be applied to 3-port or 4-port devices such as optical circulators, 1×2 or 2×2 fiber optic couplers, WDM filters, optical switches and so on.

We further extended our compact FMF collimator concept to a four-mode group fiber supporting 6 spatial modes including two spatial orientations and a pair of collimators was fabricated using a graded-index four mode-group fiber. The mode dependent coupling loss from a pair of collimators was measured as a function of working distance as shown in Fig. 3(a). Similar to the previous two-mode group fiber collimator, higher-order modes show progressively higher coupling losses than lower-order modes. However note that the MDL of the device is still reasonably small (only 0.3 dB at L=10 mm and 1.1 dB at L=30 mm) and it can be used to realize practical SDM components with low insertion loss and low MDL. We performed a Time-of-Flight measurement on the 10 km-long 4-mode group fiber in order to characterize the FMF collimator impulse response including the modal crosstalk. The trace in Fig. 3(b) shows the three main discernible mode peaks at their relative differential group delays locations (0.45 ns/km for LP_{11}, 0.60 ns/km for LP_{21}&LP_{02}). Note that LP_{21} and LP_{02} peaks are strongly mixed and a mixture of the spatial mode intensity profiles (LP_{21}&LP_{02}) was observed on a CCD at the fiber output end even though we excited only one of the modes (e.g. LP_{21}) at the fiber input end. This represents a general feature of the graded-index multimode fiber. The measured mode ER was -16.5 dB for LP_{01}, -15.1 dB for LP_{11} and -13.2 dB for LP_{21}&LP_{02}, respectively. With regard to the development of higher mode count SDM components, we expect that the device performance can be further improved by using slightly different lens choice and by adopting bulk components with a slightly larger clear aperture.

III. MULTICORE FIBER ISOLATORS

Figure 4(a) shows a schematic diagram of a representative 32-core multicore fiber (MCF) collimator assembly consisting of a cylindrical micro-optic lens and a MCF ferrule, fitted in a ferrule sleeve [9,10]. Similar to the previous few mode fiber collimators, compact micro-optic lens elements can transform the emergent light from an input 32c-MCF into a collimated free-space beam that can then be refocused into another length of MCF using a second identical assembly. Optical elements can then be inserted into the free space beam path (e.g. a bulk isolator in our experiment) to provide in-line functionality. Fig. 4(b) shows a cross-section of the 32-core MCF used in our isolator which is a heterogeneous, trench-assisted MCF incorporating a square lattice core arrangement to reduce the inherent inter-core crosstalk (XT) of the fiber. The core pitch is 29 μm and the cladding diameter is 243 μm. The measured inter-core XT of the fiber was less than -55 dB/km and the fiber has recently been used in high-density 32-core MCF transmission experiments over 1600 km [12]. To optimize the alignment of the MCF collimators, we first illuminate all 32-cores of the MCF using a single low-coherence amplified spontaneous emission (ASE) source. To enable this, the single mode source output fiber was first spliced to a short section (~3 mm) of coreless fiber (i.e. pure silica rod fiber) with the purpose of expanding the beam size and this was then spliced to the 32-core MCF. The launched optical power varies from core to core but it nevertheless allows stable and efficient simultaneous light coupling into all fibre cores. The other end of the MCF was angle-cleaved at 8^{o} to reduce Fresnel reflections, inserted into the glass ferrule and fixed

into place with UV curable adhesive. Next, the MCF ferrule was inserted into the ferrule sleeve and the distance between the C-lens and fiber ferrule was carefully adjusted to achieve an array of high quality collimated beams. As shown in Fig, 4(c), spatial interference patterns were observed in the near field from the collimator but clean thirty-two spatial mode beams were observed in the far field which remain collimated over relatively long distances (up to 50 mm) from the collimator. A pair of MCF collimators was built and mounted on a multi-axis precision micro-stage (offering translation, tilt and rotation adjustments) to align the collimators. Importantly, the MCF collimators intrinsically require rotational alignment and the far field intensity distribution from the collimator was examined using a visible He-Ne laser for rough angular alignment of the MCF collimator. We next developed a compact air-gap device based on two such collimators, configured such that we could insert and fix in place different functional elements (e.g. an isolator core in this experiment) to provide for robustly packaged MCF components. Our final packaged 32-core MCF isolator is shown in Fig. 4(d).

To characterize the integrated 32-core MCF isolator, all fiber cores were again illuminated by a single ASE source as described previously and the near field distribution of the fiber was investigated with a 2-dimentional power sampling method. A CCD camera can be used to observe the near field distribution of the fiber but we used a single mode fiber probe scanning method in the near field of the fiber to obtain a power distribution measurement with better dynamic range across the fiber cross-section. The scan area was 250 μm × 250 μm sampled on a 200 by 200 step grid in the near field plane using an SMF28 fiber with an MFD of 10.4 μm. The resulting intensity distribution is plotted on a logarithmic scale and the associated contour plot is shown in Fig. 5(a). 32 clean spatial beams from the individual cores were clearly observed and the noise floor (due to scattered light trapped in the fiber cladding) was less than -60 dB compared to the maximum beam intensity (which means that the measurable dynamic range is more than 60 dB). By comparing the spatial intensity distribution before and after our fabricated isolator, we can quantitatively evaluate the core dependent insertion loss of the device. As shown in Fig. 5(b), the average insertion loss was ~1.4 dB and the core-to-core variation was less than 1.4 dB (note that this value also includes a loss contribution from two extra splices between the MCFs and thus the actual isolator loss and core IL variation is appreciably lower). The left figure of Fig. 5(b) illustrates the measured insertion loss associated with a given core. The outer cores have relatively larger insertion losses than the inner cores which may be due to a slight angular orientation misalignment of the MCF splices and/or collimator assembly. However, one side of the outer cores shows a slightly higher insertion loss which may be due to beam clipping as a result of the limited (1 mm x 1 mm) clear aperture of the isolator core. We can expect to further improve the isolator performance, especially in terms of core-to-core IL variation using a slightly different lens choice and by adopting bulk components with a slightly larger clear aperture. In order to estimate the crosstalk (XT) between the fiber cores we carefully excited one of the cores in the central region using a spliced single mode fiber. As shown in Fig. 6(a), the XT

between the neighboring cores was less than -50 dB from the SMF-MCF splice itself. Interestingly, an unexpectedly significant level of beam intensity was also observed in the middle of core lattice. This is due to light guidance by the pure silica region surrounded by fluorine doped index trenches as evident from the fibre cross-section in Fig. 4(b). The light guidance from this region can be suppressed by bending the fiber tightly but a noise floor of around -50 dB was still observed from a 20 m section of MCF. Some of the core mode profiles exhibit an LP_{11} beam feature due to higher order mode guidance in short lengths of this fiber (the effective cutoff wavelength is 1530 nm for a 1 km length of the fiber). As shown in Fig. 6(b), incorporation of the 32-core MCF isolator increased the neighboring core XT slightly but it was still less than <-40 dB. Finally, the excited core of the MCF was then spliced to another SMF pigtail and the optical isolation and back reflection were investigated. The peak isolation was around 43 dB at 1559 nm and an optical isolation exceeding 32 dB was obtained over the entire C-band. We also measured the back reflection for the 32-core MCF isolator and a value of -32 dB was obtained over the full C-band due to the angled fiber facet. Note that the developed 32-core MCF isolators was incorporated into optical amplifier (i.e. a cladding-pumped 32-core multicore fiber amplifier) in a fully integrated format to suppress unwanted back-reflections and data transmission over a distance up to 1,850 km was successfully demonstrated for 100 Gbit/s QPSK signals in a MCF recirculating loop [13,14].

IV. CONCLUSIONS

We have successfully realized compact optical isolators for SDM systems including both few mode fibers and multicore fibers. An excellent optical performance of < 1 dB insertion loss and < 0.5 dB MDL was successfully achieved in few mode fiber isolators. The maximum peak isolation was more than 40 dB and the optical isolation over the full C-band was more than 30 dB. This micro-collimator approach can be applicable to other types of SDM fibers and a high-core count 32-core multicore fiber isolator has also been fabricated with an average insertion loss of ~1.4 dB, core-to-core variation of ~1.4 dB and an inter-core crosstalk of less than -40 dB. This indicates that the micro-optic collimator assembly concept can be extended to SDM fibers, providing the opportunity for an array of new and practical packaged components with performance, in terms of functionality and insertion loss, comparable to the equivalent existing single mode fiber devices, whilst at the same time ensuring low levels of inter-channel cross-talk.

ACKNOWLEGEMENTS

This work was supported by the EU-Japan coordinated R&D project on “Scalable And Flexible optical Architecture for Reconfigurable Infrastructure (SAFARI)” by the Ministry of Internal Affairs and Communications (MIC) of Japan and EC Horizon 2020 and by the EPSRC funded “AirGuide Photonics” Programme Grant (EP/P030181/1).

REFERENCES

1. D. J. Richardson, J. M. Fini, and L. E. Nelson, "Space-division multiplexing in optical fibres," Nat. Photonics **7**, 354–362 (2013).

2. P. J. Winzer, "Making spatial multiplexing a reality," Nat. Photonics **8**, 345–348 (2014).

3. K. Saitoh and S. Matsuo, "Multicore Fiber Technology," J. Light. Technol. **34**, 55–66 (2016).

4. R. Ryf, S. Randel, A. H. Gnauck, C. Bolle, A. Sierra, S. Mumtaz, M. Esmaeelpour, E. C. Burrows, R.-J. Essiambre, P. J. Winzer, D. W. Peckham, A. H. McCurdy, and R. Lingle, "Mode-Division Multiplexing Over 96 km of Few-Mode Fiber Using Coherent 6×6 MIMO Processing," J. Light. Technol. **30**, 521–531 (2012).

5. V. A. J. M. Sleiffer, Y. Jung, V. Veljanovski, R. G. H. van Uden, M. Kuschnerov, H. Chen, B. Inan, L. G. Nielsen, Y. Sun, D. J. Richardson, S. U. Alam, F. Poletti, J. K. Sahu, A. Dhar, A. M. J. Koonen, B. Corbett, R. Winfield, A. D. Ellis, and H. de Waardt, "73.7 Tb/s (96 ×3×256-Gb/s) mode division multiplexed DP-16QAM transmission with inline MM-EDFA," Opt. Express **20**, B428–B438 (2012).

6. Y. Jung, S. Alam, Z. Li, A. Dhar, D. Giles, I. P. Giles, J. K. Sahu, F. Poletti, L. Grüner-Nielsen, and D. J. Richardson, "First demonstration and detailed characterization of a multimode amplifier for space division multiplexed transmission systems," Opt. Express **19**, B952–B957 (2011).

7. S. Yuan and N. A. Riza, "General formula for coupling-loss characterization of single-mode fiber collimators by use of gradient-index rod lenses: errata," Appl. Opt. **38**, 6292 (1999).

8. Y. Jung, S. Alam, and D. J. Richardson, "Compact few-mode fiber collimator and associated optical components for mode division multiplexed transmission," Opt. Fiber Commun. Conf. (2016), Pap. W2A.40 W2A.40 (2016).

9. Y. Jung, S. Alam, Y. Sasaki, and D. J. Richardson, "Compact 32-core multicore fibre isolator for high-density spatial division multiplexed transmission," in *ECOC* (VDE, 2016), p. W2.B4.

10. Y. Jung, J. R. Hayes, S. U. Alam, and D. J. Richardson, "Multicore Fibre Fan-In/Fan-Out Device using Fibre Optic Collimators," in *2017 European Conference on Optical Communication (ECOC)* (IEEE, 2017), pp. 1–3.

11. T. Hayashi, T. Taru, O. Shimakawa, T. Sasaki, and E. Sasaoka, "Design and fabrication of ultra-low crosstalk and low-loss multi-core fiber," Opt. Express **19**, 16576 (2011).

12. T. Mizuno, K. Shibahara, F. Ye, Y. Sasaki, Y. Amma, K. Takenaga, Y. Jung, K. Pulverer, H. Ono, Y. Abe, M. Yamada, K. Saitoh, S. Matsuo, K. Aikawa, M. Bohn, D. J. Richardson, Y. Miyamoto, and T. Morioka, "Long-Haul Dense Space-Division Multiplexed Transmission Over Low-Crosstalk Heterogeneous 32-Core Transmission Line Using a Partial Recirculating Loop System," J. Light. Technol. **35**, 488–498 (2017).

13. S. Jain, C. Castro, Y. Jung, J. Hayes, R. Sandoghchi, T. Mizuno, Y. Sasaki, Y. Amma, Y. Miyamoto, M. Bohn, K. Pulverer, M. Nooruzzaman, T. Morioka, S. Alam, and D. J. Richardson, "32-core erbium/ytterbium-doped multicore fiber amplifier for next generation space-division multiplexed transmission system," Opt. Express **25**, 32887 (2017).

14. T. Tanaka, K. Pulverer, U. Habel, C. Castro, M. Bohn, T. Mizuno, A. Isoda, K. Shibahara, T. Inui, Y. Miyamoto, Y. Sasaki, Y. Amma, K. Aikawa, S. Jain, Y. Jung, S. Alam, D. J. Richardson, M. Nooruzzaman, and T. Morioka, "Demonstration of Single-Mode Multicore Fiber Transport Network With Crosstalk-Aware In-Service Optical Path Control," J. Light. Technol. **36**, 1451–1457 (2018).

FIGURES

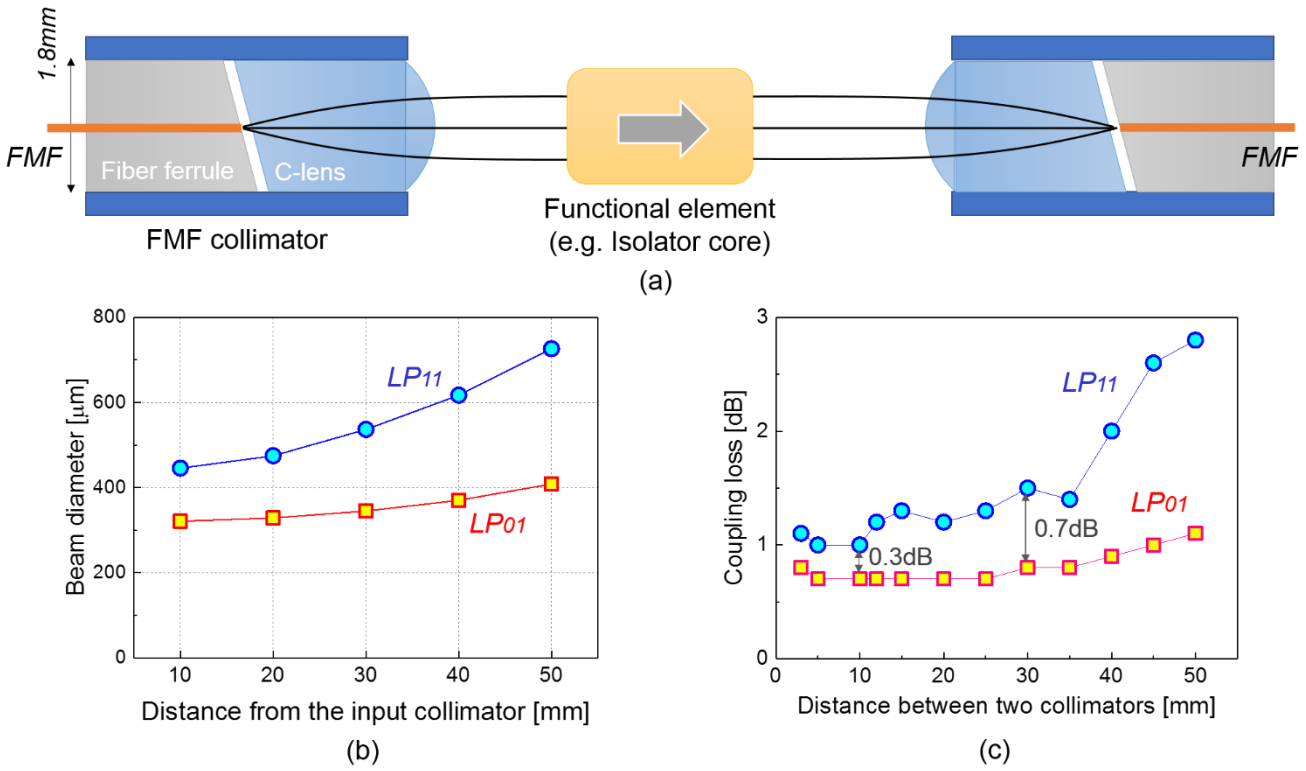

FIG. 1. (a) Schematic of a few-mode fiber (FMF) collimator assembly incorporating an optical isolator as a functional element. (b) The measured beam diameters of both LP_{01} and LP_{11} modes as a function of distance from the input fiber collimator and (c) the mode dependent coupling loss between two collimators.

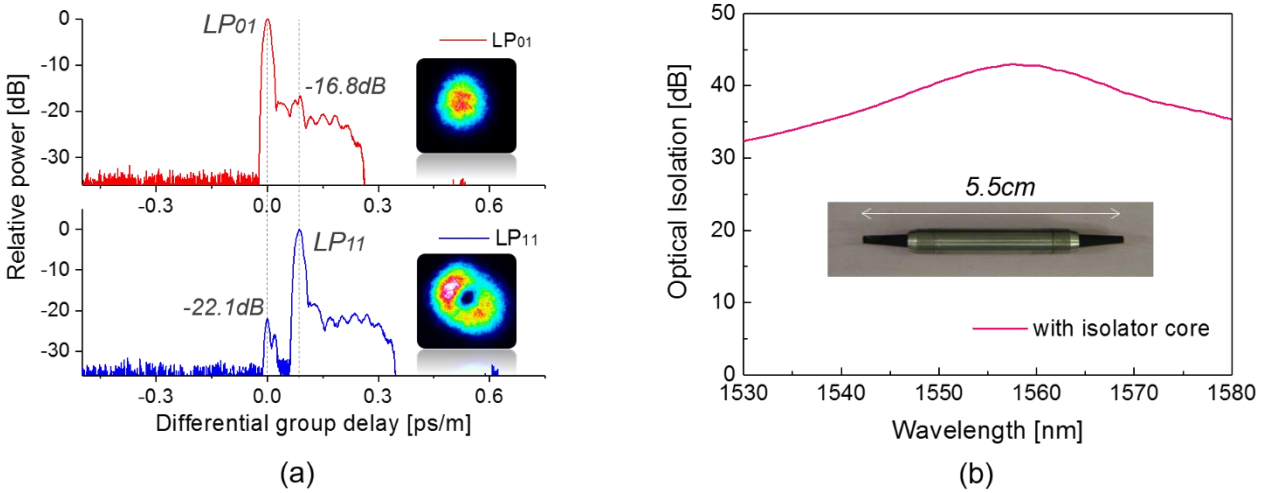

FIG. 2. (a) The estimated modal purity based on temporal impulse response measurements from a pair of FMF collimators incorporated at the input to a 10 km length of FMF and (c) optical isolation of FMF isolator.

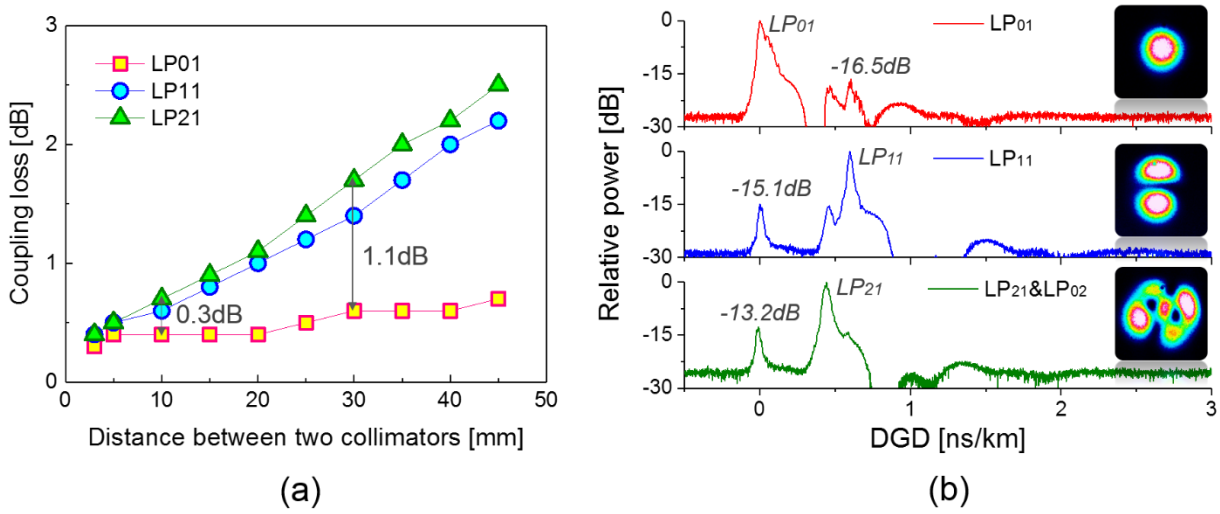

FIG. 3. (a) Mode dependent coupling loss as a function of distance between two 4-mode group fiber collimators and (b) impulse response from a pair of four mode group fiber collimators.

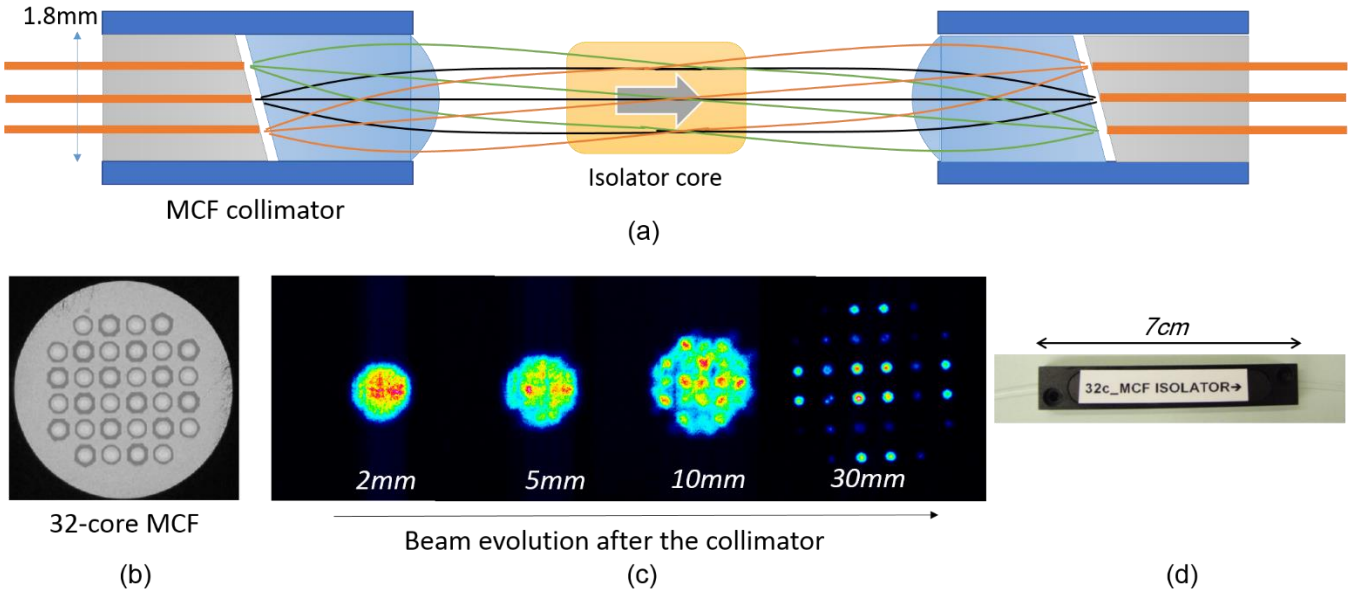

FIG. 4. (a) Schematic of a 32-core MCF isolator. (b) The cross-section of the 32-core MCF, (c) the measured beam profiles as a function of distance from the collimator and (d) the fully integrated and packaged isolator.

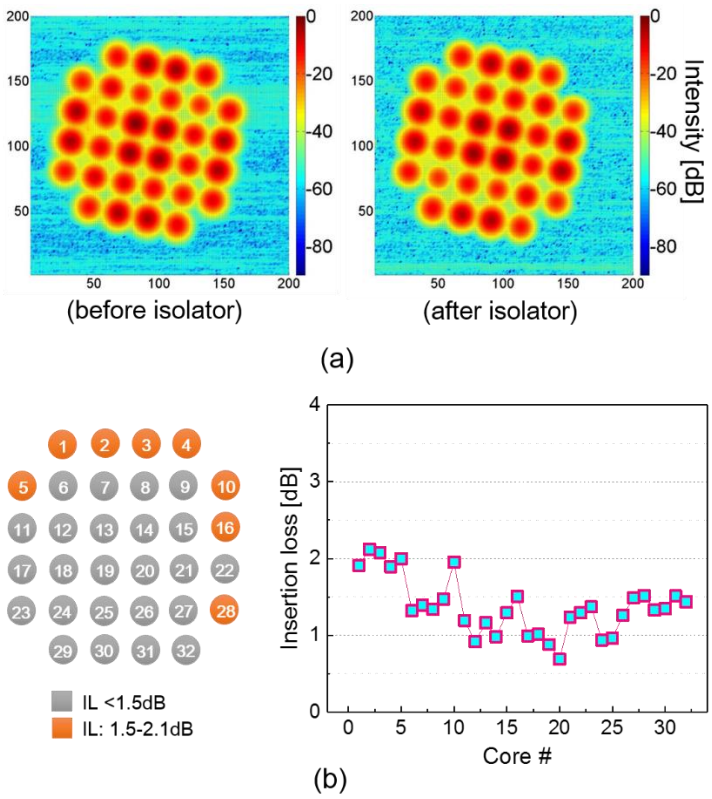

FIG. 5. (a) Measured 2-dimensional spatial beam distribution before and after the 32-core MCF isolator obtained by a power sampling method. (b) The measured core-to-core insertion loss variation of the isolator with ±0.2 dB measurement error.

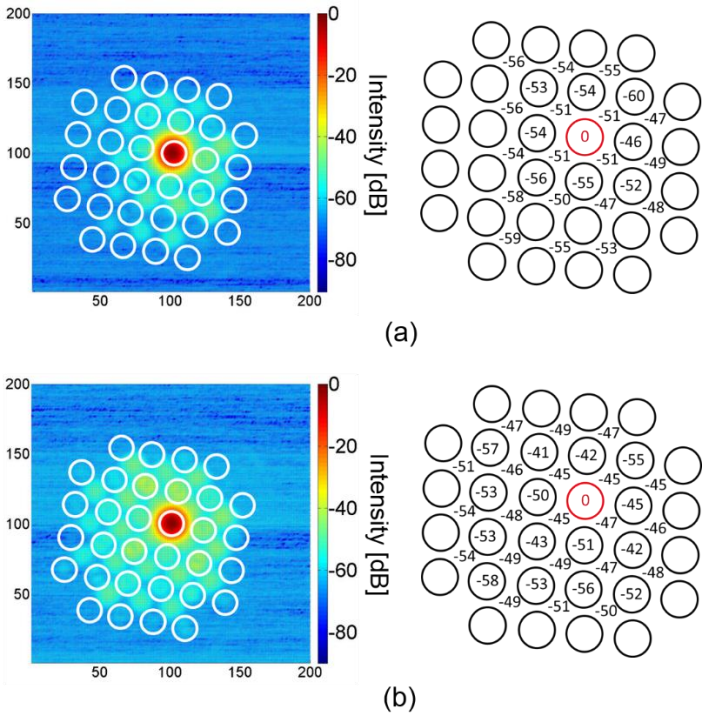

FIG. 6. Measured inter-core crosstalk contour map (a) before and (b) after 32-core MCF isolator.